

INTRODUCTION

Motivation: In the field of magnetic resonance imaging (MRI) the use of spheroids has attracted considerable interest as a block to model and predict the static magnetic fields around biological structures. MR-Osteodensitometry utilizes the inhomogeneous magnetic field within trabecular bone to gain information about its mechanical competence [1]. Such osseous networks can be modelled as arrays of spheroids with symmetry axes having various directions. The analytical solutions of magnetic spheroids in an uniform static field are well known [2]. The potential of such spheroids whose symmetry axis is the z-axis are especially derived in spheroidal coordinates. Hence, the structures of interest have to be modelled in the spheroidal system as well or the computed field values have to be subsequent transferred into the desired coordinate system.

In the current work we derived novel formulations of the potential and field for prolate and oblate spheroids. These solutions were expressed in Cartesian coordinates and enable arbitrary alignment of both the external field and the symmetry axes. Their applicability is further demonstrated via computing the field distribution within a simplified vertebra model.

METHODS

Method of solution: At first the potential and field of a homogeneous prolate or oblate spheroid in a given uniform magnetic field \mathbf{H}_0 are found in the spheroidal coordinates by separation [3]. The given and the wanted potentials are expanded in series of particular solutions of the potential equations. These solutions are products of Legendre polynomials. The boundary conditions are matched. The Legendre polynomials and functions can be expressed by elementary functions. Thereafter the solutions can be expressed in Cartesian coordinates by the transformation equations. Finally the general case with arbitrary symmetry axis \mathbf{n} was derived by decomposing the field vectors into components parallel and perpendicular to \mathbf{n} . The general expression for the reaction field in the exterior is given:

$$H_{\alpha}^{\sigma,k}(x,y,z) = \sum_{\beta=1}^3 K_{\alpha\beta}^{\sigma,k} H_{0\beta}, \quad \sigma = p, o; k = e, i$$

$$K_{\alpha\beta}^{\sigma,e}(x,y,z) = \mp x_{\alpha}^{\sigma} x_{\beta} L_1^{\sigma} \frac{u_{\sigma}(\mathbf{r}, \mathbf{n})}{w_{\sigma}(\mathbf{r}, \mathbf{n})} \frac{4}{[(u_{\sigma}(\mathbf{r}, \mathbf{n}))^2 \mp 2]^2} \pm x_{\alpha}^{\sigma} n_{\beta} (\mathbf{r} \cdot \mathbf{n}) L_1^{\sigma} \frac{4 u_{\sigma}(\mathbf{r}, \mathbf{n})}{w_{\sigma}(\mathbf{r}, \mathbf{n}) [(u_{\sigma}(\mathbf{r}, \mathbf{n}))^2 \mp 2]^2}$$

$$- \delta_{\alpha\beta} L_1^{\sigma} (f_1^{\sigma} - f_2^{\sigma}) - n_{\alpha} n_{\beta} [L_0^{\sigma} (f_1^{\sigma} - f_3^{\sigma}) - L_1^{\sigma} (f_1^{\sigma} - f_2^{\sigma})] - x_{\alpha}^{\sigma} n_{\beta} (\mathbf{r} \cdot \mathbf{n}) L_0^{\sigma} \frac{2}{[2 \mp (u_{\sigma}(\mathbf{r}, \mathbf{n}))^2] u_{\sigma}(\mathbf{r}, \mathbf{n}) w_{\sigma}(\mathbf{r}, \mathbf{n})}$$

RESULTS

Resulting field plots of a prolate spheroid modeling a single trabecula

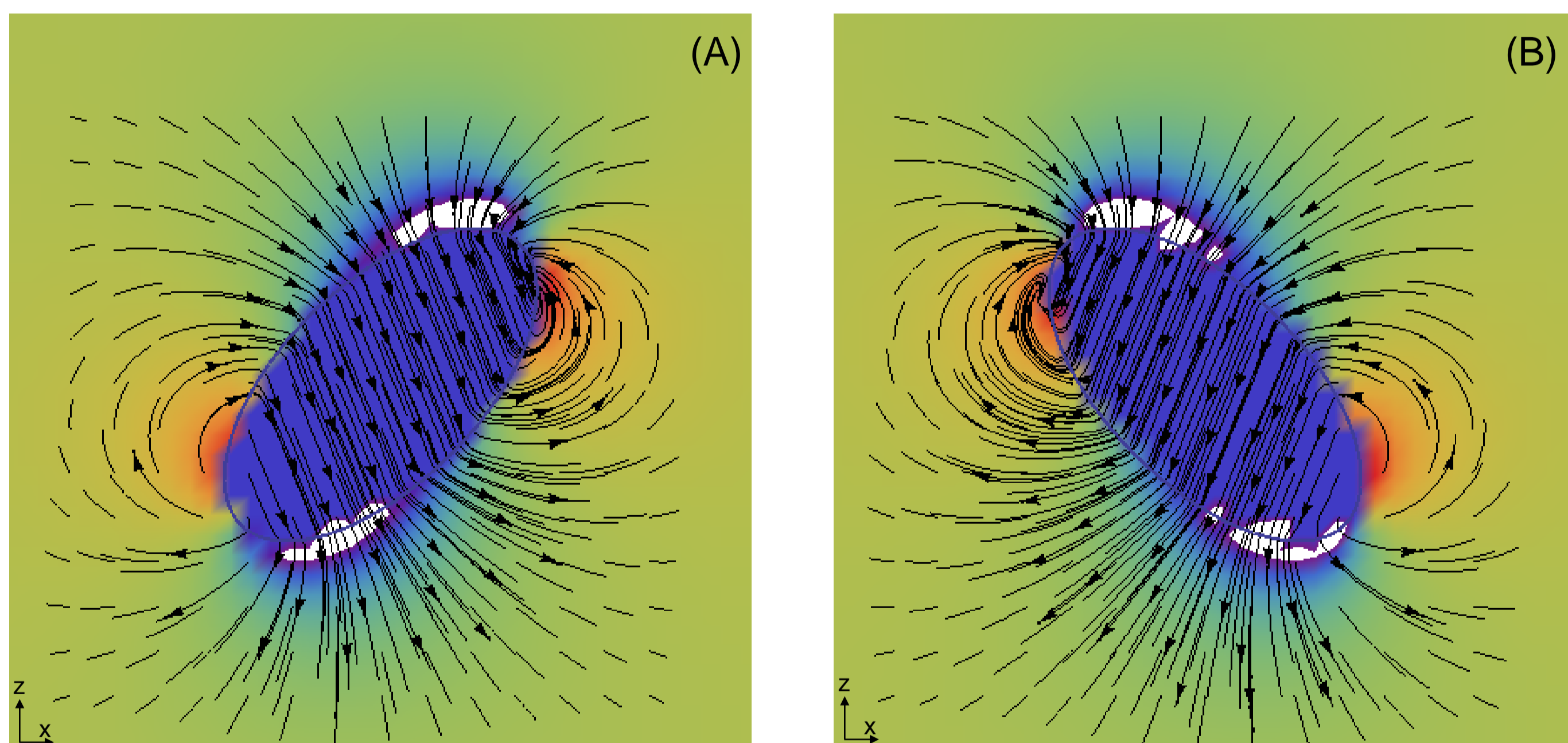


Fig. 1: Prolate spheroids in an uniform magnetic field. $H_{r1,x}(x,z)$ and $H_{r1,z}(x,z)$ were utilized to compute the field lines in the x-z plane, overlaid onto the reaction field $H_{r1,z}(x,z)$. The axial ratio of the cross sectional ellipse was 1:2. An external H_0 field was applied along the z-axis. The orientation of the main axis of the spheroid to the z-axis were set to $\pi/4$ for (A) and $-\pi/4$ for (B).

The reaction fields were computed using following parameters: $H_0 = 2.387 \times 10^6$ A/m ; the susceptibility of bone marrow $\chi_1 = -0.62 \times 4\pi \times 10^{-6}$, and bone $\chi_2 = -0.9 \times 4\pi \times 10^{-6}$.

Impact of field distortions on the MR signal within a 3D vertebra model

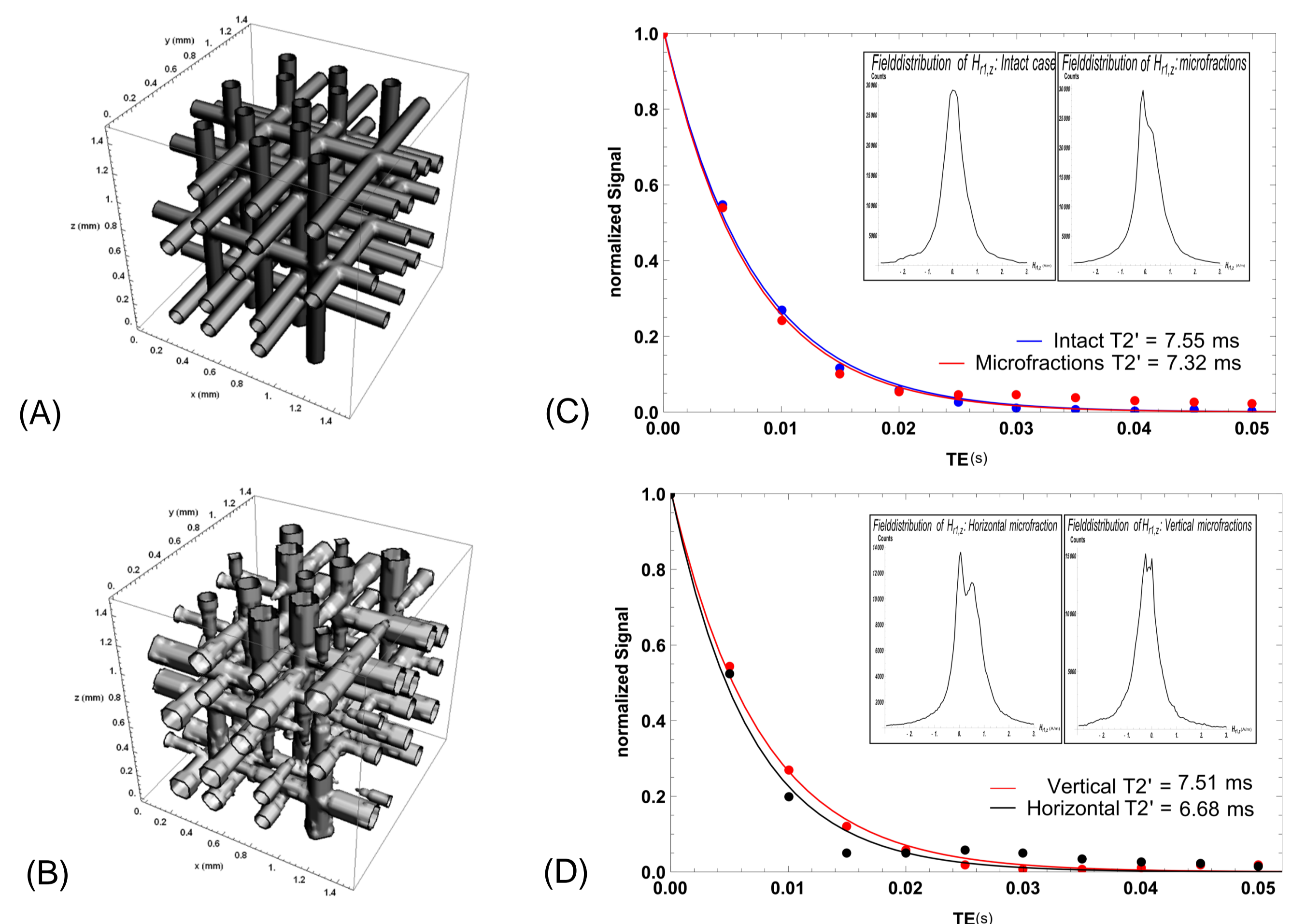


Fig. 2: (A,B) Depiction of the $1.5 \times 1.5 \times 1.5$ mm³ unit cell; the x/y/z aligned sets are built up of prolate ellipsoids with a minor axis of 240 μ m and a bone volume / total volume fraction of 15 %. (B) The trabecular micro fractures were simulated by replacing each of the intact trabeculae with two opposed shifted versions. (C) Magnetic field distribution inside the bone marrow together with the resulting approximation of the signal course to a monoexponential decay, in case of intact and total interrupted situation. (D) Field distribution and signal decay in the vicinity of the osseous network for either horizontal or vertical interrupted case.

A main magnetic field $H_0 = 2.38732 \times 10^6$ A/m with α ($\rightarrow x, z$) and β parallel z-axes ($\rightarrow y, z$) was applied.

CONCLUSION

The advantage of this new formalism is, that by superposition their individual field contributions it is very easy to model and investigate structures built from spheroids with different axes and positions. There is no need of complicated coordinate transformations. The orientation of the external field and of the symmetry axis can be arbitrary chosen.

As an application of the novel solutions we analysed the susceptibility effects in the vicinity of micro cracks utilizing a simplified vertebra model. The chosen configuration reveals, that microfractures lead to a minor field variation effect, whereby the resulting signal time course deviates from the monoexponential behaviour.

In general, within vertebrae affected by pathologies such as osteoporosis horizontally arranged structures get typically interrupted at first. The novel expressions make it possible to study the bone rarefaction along such pathologies. Whereby the crucial fields next to cracks of either horizontally, vertically or arbitrary orientated structures are accessible for modelling.

References: [1] Wehrli et al.: NMR in Biomed 19: 731-764 (2006), [2] Landau and Lifshitz: Pergamon Press (1960), [3] Kuchel et al.: NMR in Biomed 2:151-160 (1989), [4] Kraiger et al.: COMPEL 32:936-960 (2013), [5] Kraiger et al. Institute for Theoretical and Computational Physics <http://itp.tugraz.at/~schnizer/MedicalPhysics/>